$GEANT\,4$ SIMULATION OF NEUTRON TRANSPORT AND SCATTERING IN MEDIA

$O.S.\,Deiev^*$

National Science Center "Kharkov Institute of Physics and Technology", 61108, Kharkov, Ukraine

(Received December 27, 2012)

$GEANT\,4$ simulation toolkit and $PhysList\ QGSP\ BIC\ HP$ for simulate neutron transport and scattering was used. Primary neutron spectrum was modeled similar spectrum of $^{239}Pu - Be(\alpha, n)$ neutron source. Spectra of neutron passing through the material and scattered were obtained. Number of thermal neutrons after passing various materials were calculated. Detector-dosimeter $MKS-01R$ was used for measurements of the experimental thermal neutron flux from $^{239}Pu - Be(\alpha, n)$ neutron source. Satisfactory agreement between calculations and experiment was obtained.

PACS: $28.20.\mathrm{Gd}, 07.05.\mathrm{Tp}$

1. INTRODUCTION

In all studies and applications using neutrons, calculations of neutron transport in matter are of the fundamental importance. Simulation is necessary to estimate the flux of neutrons traversing from materials and the energy loss in the materials, to determinate the energy distribution of the emerging neutrons, to calculate the shielding and moderator, ets. Monte-Carlo simulations are often usefully in studying the response of neutron detectors employed in low-, intermediate-, and high- energy physics, as well as to estimate the activity induced in different detectors by the intense neutron fields. Finally, neutron transport calculations based on Monte-Carlo method are becoming basic tools in radiation protection dosimetry of a neutron or mixed radiation fields, as they help to link measurable observables with radiation protection quantities. $GEANT\,4$ high-energy physics simulation toolkit [1] widely used to simulate neutron scattering and propagation [2, 3, 4, 5] and modeling of neutron detectors [6, 7].

In this paper $PhysList\ QGSP\ BIC\ HP$ (which includes $NeutronHPElastic,\ NeutronHPInelastic,\ NeutronHPCapture,\ NeutronHPFission$) was used to simulate the interaction of neutrons with the material. Primary neutron spectrum was modeled similar spectra of $^{239}Pu - Be(\alpha, n)$ neutron source. Purpose of this study was to estimate the number of thermal neutrons after passing of a different materials. In future these thermal neutrons are supposed to use for initialization of the reaction $Gd(n, \gamma e^-)$ [6, 7].

2. RESULTS OF MODELING

2.1. Neutron transport through a plate

For testing neutron transport through a plates of material we used simple geometry. Monoenergetic neutrons with energy $E_0 = 10^{-3}$, 1 and $10^3\,keV$ emitted from a point-like source are propagating through a square plates with surface $50 \times 50\,cm^2$, positioned at the distance $10\,cm$ from the source. Trajectories of the particles are directed perpendicular to the surface. On the opposite side of the plate the sphere of $30\,cm$ radius is used to determine the fluence and energy distribution of the emerging neutrons. The flux of neutrons energy En passing through the plate of two materials Fe and $CONCRETE$ thickness t normalized to the incident flux I_{plate}/I_0 (I_{plate} is intensity of beam passing through the plate, I_0 is intensity of the primary beam) is shown in Table I. The results are close to the calculations [2].

Table 1. *The normalized flux of neutrons energy $E_0 = 10^{-3}$, 1 and $10^3\,keV$ passing through the Fe and $CONCRETE$ plate thickness (t, cm)*

E_0, keV	10^{-3}	1	10^3
$Fe, 5\,cm$	0.65	0.33	0.14
$Fe, 10\,cm$	0.4	0.17	0.022
$Fe, 20\,cm$	0.2	0.035	0.00032
$CONCRETE, 10\,cm$	0.22	0.28	0.32
$CONCRETE, 20\,cm$	0.08	0.095	0.12

Neutrons with energy $E_0 = 2\,MeV$ passing through a flat plate of polyethylene were calculated ($POLYETHYLENE$, C_2H_4, $\rho = 0.94\,g/cm^{-3}$) in the same geometry. Neutrons passing forward (in the forward hemisphere) and gamma rays in 4π geometry were detected. For polyethylene $5\,cm$ thickness the normalized flux of thermal neutrons with $E_n < 1\,eV$ was 0.082, with $E_n < 0.1\,eV$ was 0.064. Calculation of neutron lethargy was performed on formula $U = ln(E_0/E_n)$, ratio of the neutrons number in the lethargy interval $U(0; 2.3)/U(15.9; 18.2)=6.5$, which is close to the results [8].

*Corresponding author E-mail address: deev@kipt.kharkov.ua

2.2. Neutron transport through a sphere

Transport of neutrons through paraffin sphere was calculated. Neutron spectra in 4π geometry were calculated. Point neutron source was located inside the sphere of radius R of the material $PARAFFIN$. Neutrons with initial energy $E_0 = 1$, 5 and 11 MeV passed through the sphere in random direction were registered. Typical neutrons trajectory from the center of paraffin sphere are presented in Fig. 1.
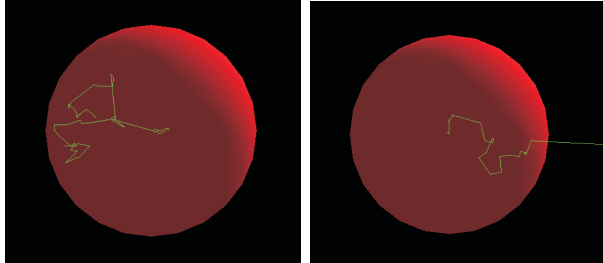
Fig. 1. *Trajectory of neutrons $E_0 = 1\,MeV$ from the center of paraffin sphere diameter $20\,cm$. Neutron trajectory (left) and slow neutron trajectory with capture reaction and gamma-ray emission (right)*

The neutrons on the surface of the sphere were detected. Gamma radiation passed through sphere, and then registered on the larger diameter sphere. Normalized flux through the spherical surface of the thermal neutrons $E_n < 0.1\,eV$, $< 0.025\,eV$ for the initial neutron energy $E_0 = 1$, 5 and 11 MeV were calculated depending on radius paraffin sphere. The total number of thermal neutrons decreases with increasing initial energy E_0. Maximum of the thermal neutrons distribution is depending on the radius of the sphere: 10, 12 and 15 cm for $E_0 = 1$, 5 and 11 MeV, respectively. In Fig. 2 flux through the spherical surface of neutrons with energy E_0 and the total flux neutrons as the function of the paraffin sphere radius are shown. Initial neutron energy $E_0 = 1$, 5 and 11 MeV.
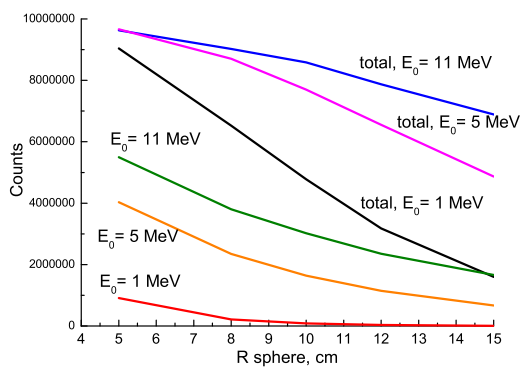

Fig. 2. *Flux of neutrons with energy E_0 (green, orange, red) and the total flux (blue, pink, black) neutrons as the function of the paraffin sphere radius R, cm. Initial neutron energy $E_0 = 1$, 5 and 11 MeV ($N_n = 10^7$)*

The total flux of neutrons decreases with increasing radius sphere and with the decrease of the initial energy. However, even for $R = 50\,cm$ at $E_0 = 11\,MeV$ through sphere penetrates 0.2 percent of the neutrons with initial energy E_0.
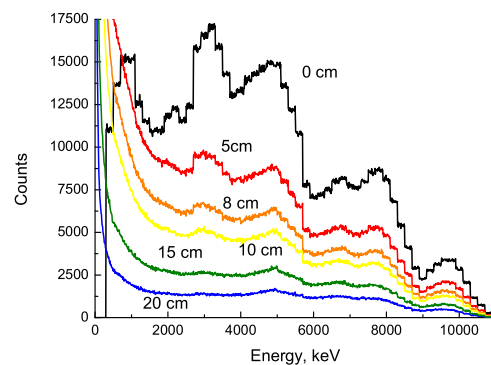
2.3. Modeling neutron spectrum similar spectrum of $^{239}Pu - Be(\alpha, n)$ neutron source

Neutron spectrum which similar to the emission of $^{239}Pu - Be(\alpha, n)$ source [9] was simulated by Monte Carlo method (Fig. 3). In work [9] neutron spectra have been measured for $^{239}Pu - Be(\alpha, n)$ sources containing 2, 14, 80 and 160 g of ^{239}Pu. Intensity maxima near 1.4, 2.0, 3.1, 4.8, 6.6, 7.7 and 9.8 MeV were seen in all spectra. The stilbene crystal for fast neutron spectrometer and a long counter were used in these measurements [9].
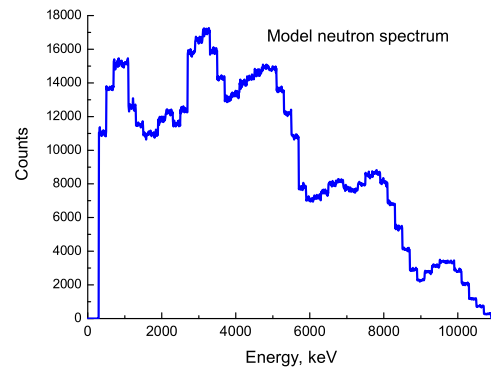
Fig. 3. *Primary neutron spectrum modeled similar spectrum of $^{239}Pu - Be(\alpha, n)$ neutron source [9]*

The neutron spectra for $PhysList\ QGSP\ BIC\ HP$ in 4π geometry were calculated (Fig. 4). The neutron energy decreases due to the scattering on nuclei C and H. The registered spectrum is shifting to the range of the thermal neutron energy with increasing radius (R, cm) of the sphere.

Fig. 4. *The neutron spectra in 4π geometry for different R, cm. Primary neutron spectrum (black) modeled similar spectrum of $^{239}Pu - Be(\alpha, n)$ neutron source*

Some of the results obtained for the primary neutron spectrum modeled similar spectrum of $^{239}Pu - Be(\alpha, n)$ neutron source are presented below. Polyethylene layers and spheres of polyethylene

paraffin, water, carbon were used as moderators. Neutrons passed in the forward hemisphere were registered for case of the plate of material. The neutrons were detected in 4π geometry for case a sphere. The characteristic line with $E_\gamma = 2.223\,MeV$ were appeared in the spectra of gamma rays. This line corresponds to the thermal neutron capture $^1H(n,\gamma)^2H$, i.e. the large proportion of thermalized neutrons is reacted capture and disappears. There is also the line with $E_\gamma = 4.438\,MeV$, which corresponds to the inelastic scattering of $^{12}C(n, n'\gamma)^{12}C$. Normalized flux of thermal neutrons with $E_n < 0.1\,eV$, $< 0.025\,eV$ and gamma quanta with $E_\gamma = 2.223$ and $4.438\,MeV$ after passing through the layer of polyethylene are given in Table 2.

Table 2. *Normalized flux of thermal neutrons with $E_n^1 < 0.1\,eV$, $E_n^2 < 0.025\,eV$ and gamma quanta with $E_\gamma^1 = 2.223$ and $E_\gamma^2 = 4.438\,MeV$ after passing through the layer of polyethylene*

t, cm	E_n^1	E_n^2	E_γ^1	E_γ^2
5	0.046	0.013	0.026	0.0027
10	0.084	0.024	0.126	0.0027
12	0.079	0.023	0.159	0.0024
15	0.064	0.018	0.193	0.0019

The energy distribution of the thermal neutron corresponds to the known Maxwell curve with a maximum of kT $0.025\,eV$ (Fig. 5). The maximum number of thermal neutrons after passing a polyethylene plate $10\,cm$ is observed. Further increase thickness does not increase the number of thermal neutrons due to thermal neutron capture reaction $^1H(n,\gamma)^2H$. Correspondingly the yield of gamma rays with $E_\gamma = 2.223\,MeV$ increased.
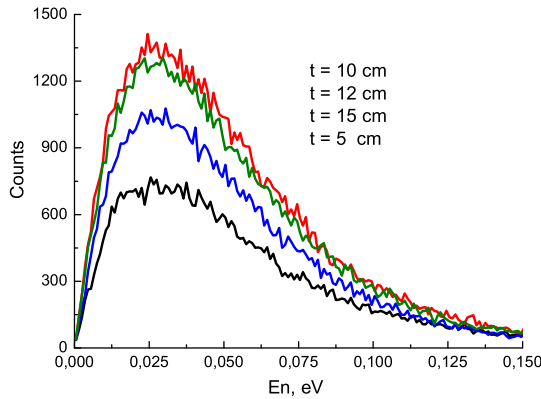
Fig.5. *The energy distribution of the thermal neutron after passing through a layer of polyethylene (t, cm, $N_n = 10^6$)*

Basic results of the neutrons thermalization passing the polyethylene sphere are shown in Table 3 and for paraffin sphere are shown in Table 4. Maximum thermal neutrons is achieved at the sphere radius $R \sim 10...11\,cm$. Normalized flux of thermal neutrons with $E_n < 0.1\,eV$, $< 0.025\,eV$ and gamma quanta with $E_\gamma = 2.223$ and $6.13\,MeV$ (re-

action $^1H(n,\gamma)^2H$ and $^{16}O(n, n'\gamma)^{16}O$) after passing through the water sphere are given in Table 5.

Table 3. *Normalized flux of thermal neutrons with $E_n^1 < 0.1\,eV$, $E_n^2 < 0.025\,eV$ and gamma quanta with $E_\gamma^1 = 2.223$ and $E_\gamma^2 = 4.438\,MeV$ after passing through the polyethylene sphere $R\,cm$)*

R, cm	E_n^1	E_n^2	E_γ^1	E_γ^2
5	0.071	0.02	0.019	0.0058
10	0.19	0.054	0.16	0.0059
12	0.188	0.053	0.23	0.0056
15	0.157	0.044	0.31	0.0044

Table 4. *Normalized flux of thermal neutrons with $E_n^1 < 0.1\,eV$, $E_n^2 < 0.025\,eV$ and gamma quanta with $E_\gamma^1 = 2.223$ and $E_\gamma^2 = 4.438\,MeV$ after passing through a paraffin sphere $R\,cm$)*

R, cm	E_n^1	E_n^2	E_γ^1	E_γ^2
5	0.071	0.019	0.020	0.005
8	0.163	0.046	0.100	0.006
10	0.188	0.055	0.171	0.006
11	0.190	0.053	0.204	0.006
12	0.187	0.054	0.234	0.005
15	0.155	0.045	0.307	0.004
20	0.09	0.026	0.349	0.002

Maximum thermal neutrons flux is achieved at the sphere radius R $15\,cm$. Normalized flux of thermal neutrons with $E_n < 1\,eV$, $< 0.25\,eV$, $E_n < 0.1\,eV$, $< 0.025\,eV$ after passing through a carbon sphere are given in Table 6. The advantage of the carbon sphere is not a strong thermal neutron capture. Disadvantage is the large thickness necessary for thermalization of neutrons.

Table 5. *Normalized flux of thermal neutrons with $E_n^1 < 0.1\,eV$, $E_n^2 < 0.025\,eV$ and gamma quanta with $E_\gamma^1 = 2.223$ and $E_\gamma^2 = 6.13\,MeV$ after passing through the water sphere $R\,cm$*

R, cm	E_n^1	E_n^2	E_γ^1	E_γ^2
10	0.171	0.048	0.093	0.0032
15	0.187	0.054	0.211	0.0026
20	0.136	0.039	0.274	0.0019
40	0.175	0.005	0.188	0.0012

Table 6. *Normalized flux of thermal neutrons with $E_n^1 < 1\,eV$, $E_n^2 < 0.25\,eV$, $E_n^3 < 0.1\,eV$, $E_n^4 < 0.025\,eV$ after passing through a carbon sphere $R\,cm$*

R, cm	E_n^1	E_n^2	E_n^3	E_n^4
10	0	0	0	0
20	0.034	0.025	0.020	0.010
40	0.464	0.430	0.400	0.214
60	0.675	0.660	0.634	0.360

Calculating normalized flux of thermal neutrons $E_n < 0.1\,eV$ for the mylar sphere radius of $10\,cm$ is 0.102, which is significantly worse than for polyethylene, paraffin and water. The normalized flux

from the lead sphere $R = 60\,cm$ is about 10^{-5} for neutrons with $E_n < 0.1\,eV$, but about 0.06 for neutrons $E_n < 5\,keV$. The total normalized flux of thermal neutrons with energy $E_n < 0.1\,eV$ on the surface of the paraffin sphere with radius $11\,cm$ is equal to 0.19. Accordingly, maximum number of thermal neutrons getting on the planar $Si\,PIN$-detector $1.8 \times 1.8\,mm^2$ size at intensity $^{239}Pu-Be(\alpha, n)$ source $10^6\,n \times s^{-1}$, is about $4\,n \times s^{-1}$ for $E_n < 0.1\,eV$ and for $E_n < 0.025\,eV$ about $1.1\,n \times s^{-1}$.

For testing our calculations neutron flux measurements was performed with using of the industrially manufactured neutron detector-dosimeter $MKS-01R$ and the plutonium-beryllium neutron source with the $1.13 \times 10^5\,n \times s^{-1}$ fluency. The neutron flux measurements were performed for two neutron energy ranges: $E_n < 0.025\,eV$ (thermal) and $E_n > 0.025\,eV$ (intermediate and fast). After passing through $11\,cm$ of paraffine experimental thermal neutron fluency was $4.7\,n \times cm^{-2} \times s^{-1}$. The calculated fluency of thermal neutrons is qual to $3.96\,n \times cm^{-2} \times s^{-1}$. After passing through $10\,cm$ of paraffine experimental thermal neutron flux 4.96, calculated $4.95\,n \times cm^{-2} \times s^{-1}$. After passing through 20 cm of paraffine experimental thermal neutron flux 0.63, calculated 0.59 $n \times cm^{-2} \times s^{-1}$. It is known that the $^{239}Pu-Be(\alpha, n)$ source emits background gamma quanta [11]. Geometry of calculations in which two boxes of paraffin $(10 \times 10 \times 10\,cm^3)$ and lead $(10 \times 10 \times 4\,cm^3)$ are located near to each other was used. Neutrons from the $^{239}Pu - Be(\alpha, n)$ source falls normally to the front paraffin box. Rectangular parallelepiped of paraffin thermalized the neutrons. Lead box cuts background gamma rays. The calculated flux of thermal neutrons with $E_n < 0.025\,eV$ on the back side of the Pb box was equal to $1.58\,n \times cm^{-2} \times s^{-1}$ for the source $1.13 \times 10^5\,n \times s^{-1}$. Experimental thermal neutron flux was $1.8\,n \times cm^{-2} \times s^{-1}$. Thus, the experimental data are slightly higher than the calculated values. In part this may be due to the scattering of thermal neutrons by atoms of the environment.

2.4. Thermal neutron scattering

The double change the number of thermal neutrons were experimentally registered depending on things that surround the neutron source. The number of neutrons in detector increased in presence bottles of water placed around detector. Thus, there is a reflection of thermal neutrons. Transmission and reflection (in the front and back hemisphere) neutrons of $E_n < 0.025\,eV$ for different layer materials were calculated. Some calculations in the approximation $QGSP$ were performed ($PhysList$ includes $G4HadronElastic$, $G4LENeutronInelastic$, $G4Lcapture$). Fig. 6 shows the spectra of neutron with $E_n = 0.025\,eV$ forth and scattering back (in the front and back hemisphere) in the approximation $QGSP$. The spectrum of neutrons passed forth has the sharp edge energy at $0.025\,eV$. The spec-

trum of backscattered neutrons is shifted on energy to the left according to the kinematics of the collision. Thus, the calculations in the $QGSP$ accurately to take account the kinematics of collisions. Energy of particles is accurately determined by simple formulas [10]. However, the numerical result is incorrect and different from calculations in the approximation $PhysList\,QGSP\,BIC\,HP$.
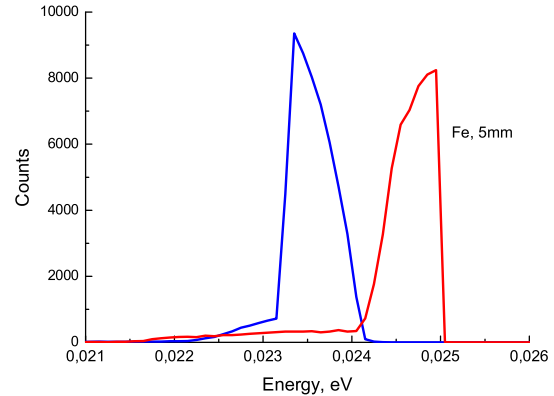
Fig. 6. *Spectra of neutron with $E_n = 0.025\,eV$ forth and scattering back (in the front (red curve) and back (blue curve) hemisphere) in the approximation QGSP*

Spectrum of backscattered neutrons calculated in the $PhysList\,QGSP\,BIC\,HP$ approximation have a different view depending from the material (Fig. 7). Thickness of targets $20\,mm$, $E_n = 0.025\,eV$, $N_n = 10^5$.
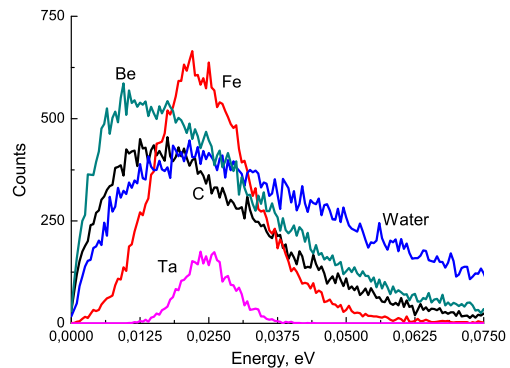
Fig. 7. *Spectra of backscattering neutron (in the back hemisphere)*

The results of the calculations are shown in Table 7. These data are close to the results of [10].

Table 7. *Normalized number of scattering neutron (in the back and forward hemisphere) $PhysList\,QGSP\,BIC\,HP$ ($E_n = 0.025\,eV$)*

t, mm	Fe, 40	Fe, 20	Fe, 10	H_2O, 50	H_2O, 20
Back	0.287	0.273	0.227	0.624	0.447
Forward	0.047	0.231	0.488	0.180	0.411
t, mm	Ta, 10	C, 20	C, 10	Be, 20	Pb, 20
Back	0.034	0.306	0.178	0.408	0.262
Forward	0.296	0.690	0.823	0.580	0.711

Note that, for example, for water the total amount back and forth scattering neutrons plus gamma with $E_\gamma = 2.223\,MeV$ were incident neutrons $N_n = 10^5$. Calculations for B, Cd, Gd-containing compounds were showed: 0 passed forward neutrons and backscattering neutrons < 50 for $N_n = 10^5$.

2.5. Nuclear reaction natural $Gd(n,\gamma\,e^-)$ yields in $GEANT\,4$

The calculation in $GEANT\,4$ ($PhysList$ $QGSP\,BIC\,HP$) gamma quanta spectrum from nuclear reaction natural $Gd(n,\gamma\,e^-)$ were performed. Yield of gamma rays is depending highly from the neutron energy and decreases with energy increasing. In Fig. 8 the yield of photons in 4π geometry for $10\,\mu m$ Gd foil and neutrons $E_n = 0.025\,eV$ and $0.25\,eV$ are presented.
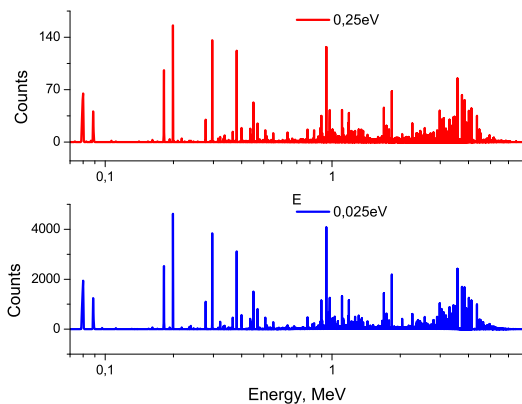
Fig. 8. *The yield of photons in 4π geometry for $10\,\mu m$ foil Gd and neutrons $E_n = 0.025\,eV$ and $0.25\,eV$ ($N_n = 10^5$)*

In Fig. 9 shows the calculated spectrum of the conversion electrons in a similar geometry.
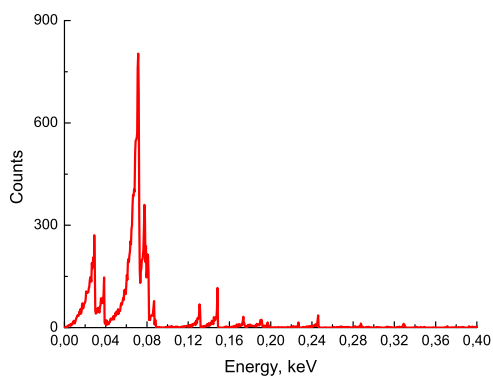
Fig. 9. *The yield of electron in 4π geometry for $10\,\mu m$ foil Gd for neutrons $E_n = 0.025\,eV$*

3. CONCLUSIONS

The interaction of neutrons with the material using $GEANT\,4$ and $PhysList\,QGSP\,BIC\,HP$ was studied. Primary neutron spectrum was modeled similar spectrum of $^{239}Pu - Be(\alpha, n)$ neutron source. The number of thermal neutrons after passing of

the different materials were calculated. Detector-dosimeter $MKS - 01R$ was used for the measurements of experimental thermal neutron flux. Agreement between calculations and experiment was satisfactory. The calculation gamma quanta and conversion electrons from nuclear reaction $Gd(n,\gamma e^-)$ for the natural isotopic composition of Gd were performed. Thermal neutrons is supposed to use to initiate this reaction. Results of this study will be used in the construction of the $SiPIN$ detector coated with the gadolinium foil for thermal neutrons registration.

References

1. *Geant*4: a toolkit for the simulation of the passage of particles through matter. CERN - the European Organization for Nuclear Research, 2011. *http://www.geant4.org/geant4/*

2. N. Colonna, S. Altieri. Simulations of neutron transport at low energy: a comparison between $GEANT$ and $MCNP$ //Health Phys. 2002, v. 82(6), p. 840-6.

3. F. Atchison, T. Brys, M. Daum, P. Fierlinger, A. Fomin, R. Henneck, K. Kirch, M. Kusniak, A. Pichlmaier. The simulation of ultracold neutron experiments using $GEANT$4 //Nuclear Instruments and Methods in Physics Research Section A: Accelerators, Spectrometers, Detectors and Associated Equipment. 2005, v. 552(3), p. 513-521.

4. Andrew Voyles, Haori Yang and Tatjana Jevremovic, University of Utah, Salt Lake City, UT. $GEANT$4 Simulation of Irradiation Facilities and Neutron Sources At University of Utah TRIGA for Nuclear Forensics and Detection //https://aiche.confex.com/aiche/2011/webprogrampreliminary/Paper237489.html

5. R. Lemrani, M. Robinson, V.A. Kudryavtsev, M.De Jesus, G. Gerbier, N.J.C. Spooner. Low-energy neutron propagation in $MCNPX$ and $GEANT$4 //Nuclear Instruments and Methods in Physics Research. Section A: Accelerators, Spectrometers, Detectors and Associated Equipment 2006, v. 560, iss. 2, p. 454-459.

6. D.A. Abdushukurov, A.A. Dzhuraev, S.S. Evteeva, P.P. Kovalenko, V.A. Leskin, V.A. Nikolaev, R.F. Sirodzhi, F.B. Umarov. Model calculation of efficiency of gadolinium-based converters of thermal neutrons. //Nuc. Instr. and Meth. B. 1994, v. 84, iss. 3, p. 400-404.

7. M. Jamil, Hyun Yong Jo, J.T. Rhee and Y.J. Jeon. Simulation study using $GEANT$4 Monte Carlo code for a Gd-coated resistive plate chamber as a thermal neutron detector

//*Radiation Measurements.* 2010, v. 45, iss. 7, p. 840-843.

8. A.Yu. Buki, S.A. Kalenik. A simple model of neutron transport and its application for the calculation of the response functions for the ball neutron spectrometr //*Journal of Kharkiv University, physical series "Nuclei, Particles, Fields"*, iss. 1/53/, N991, 2012, p. 23-27.

9. M.E. Anderson, R.A. Neff. Neutron energy spectra of different size $^{239}Pu - Be(\alpha, n)$ sources // *Nuclear Instruments and Methods*, 1972, v. 99, iss. 2, p. 231-235.

10. Rachanee Rujiwarodom, Burin Asavapibhop and Pat Sangpeng. A Simulation of Neutron Scattering via *Geant*4 //*Kasetsart journal: natural science*, 2009, v. 043, iss. 4, p. 817-821.

11. D.V. Kutniy, V.E. Kutniy, N.P. Odeychuk, et al. Use of the active well coincidence counter for the semiconductor neutron detector development //*Journal of Kharkiv University, physical series "Nuclei, Particles, Fields"*, 2008, iss. 3/39/, N823, p. 71-77.

МОДЕЛИРОВАНИЕ В $GEANT\,4$ ПЕРЕНОСА И РАССЕЯНИЯ НЕЙТРОНОВ В СРЕДАХ

А.С. Деев

Расчетный код $GEANT\,4$ и физический лист $QGSP\,BIC\,HP$ использовались для моделирования транспорта и рассеяния нейтронов. Получены спектры нейтронов, проходящих через слои материала и отраженных назад. Первичный спектр нейтронов моделируется как у источника $^{239}Pu - Be(\alpha, n)$. Рассчитаны количества тепловых нейтронов после прохождения различных материалов. Для экспериментального измерения теплового потока нейтронов использован детектор-дозиметр МКС-01Р. Согласие между расчетами и экспериментом удовлетворительное.

МОДЕЛЮВАННЯ В $GEANT\,4$ ПЕРЕНОСУ І РОЗСІЯННЯ НЕЙТРОНІВ В СЕРЕДОВИЩАХ

О.С. Деєв

Розрахунковий код $GEANT\,4$ і фізичний лист $QGSP\,BIC\,HP$ використовувались для моделювання транспорту і розсіяння нейтронів. Отримані спектри нейтронів, що проходять через шари матеріалу і розсіяних назад. Первинний спектр нейтронів моделюється як у джерела $^{239}Pu - Be(\alpha, n)$. Розраховані кількості теплових нейтронів після проходження різних матеріалів. Для експериментального вимірювання теплового потоку нейтронів використаний детектор-дозиметр МКС-01Р. Згода між розрахунками і експериментом задовільна.